CHAPTER 39

TERRESTRIAL PHOTOGRAMMETRIC MEASUREMENTS OF BREAKING WAVES AND LONGSHORE CURRENTS IN THE NEARSHORE ZONE[1]

Joseph W. Maresca, Jr.[2] and Erwin Seibel[3]

I. INTRODUCTION

We conducted a study to determine the feasibility of shore-based, oblique photographic monitoring of breaking waves, water levels, and currents within the surf zone. The purpose of this paper is to describe a new method of oblique single-image and stereoscopic-image analysis, the potential errors, and the types of measurements that can be made in the surf zone. Examples of application are presented to demonstrate the technique. Sophisticated photographic equipment is not required to collect, analyze, and interpret the data. The analysis and error discussions are directed toward the problems encountered using common equipment.

Vertical images from aircraft, helicopters, and balloons have been used in the past to study shoreline changes,[1] directional ocean-wave spectra,[2] and longshore currents.[3] Oblique images taken from the bridge of a ship have been successfully used to measure whitecap coverage under different wind speeds.[4] Terrestrial oblique images have been used to study longshore currents,[5] ice-ridge formation and breakup,[6,7] and beach changes.[8]

Oblique images, taken with a 35-mm single-lens reflex camera from an elevated point such as a bluff, are particularly suitable for the measurement of breaking waves, water level, beach run-up, and current in the surf zone under storm conditions. In contrast to other techniques of monitoring the surf zone, the photographic technique described in this paper is simple to install, reliable, accurate, and inexpensive. It can be used in all weather conditions, and the analysis of the images is simple. Both stereoscopic and single oblique images can be analyzed, depending on the specific needs and existing environmental conditions. Since the scale of an oblique photograph changes with increasing distance from the camera, the technique is limited in range to about 250 m for a cliff approximately 8 m above the mean water level. Accuracies to within 1% in the horizontal plane and better than 10% in the vertical plane are achievable at this distance.

---

1. Contribution No. 209 of The Great Lakes Research Division, The University of Michigan, Ann Arbor, Michigan 48104.
2. Stanford Research Institute, Menlo Park, California 94025.
3. University of Michigan, Ann Arbor, Michigan 48104.

Higher accuracies are obtained as distance from cliff to camera decreases. The unique feature of the oblique image is that it provides a method of delineating changes in space and time without the need for an expensive array of instruments.

II. EXPERIMENTAL METHOD

No special equipment is required for taking the oblique images. If stereoscopic oblique images are required, two 35-mm single-lens reflex cameras can be used. The cameras should be tripod-mounted and separated by a known distance. Polarizing filters are useful to decrease the glare from the water surface. In this study, stereoscopic measurements were taken along the California coast by two cameras placed 8 m apart and 8 m above the mean water level. The focal lengths of the cameras' lenses were 50 mm. The nominal focal length is sufficient for analysis. Although the simultaneous camera exposures could be taken using a long shutter release, we took the exposure by voice command. The two exposures were found to be visually identical, so no more elaborate method was pursued. Kodachrome II color slide film (ASA 25) was used. The color film is necessary for easy identification of points on the image. Slides are necessary, since they can be projected on a screen and enlarged sufficiently until points can be easily identified.

Single and stereoscopic oblique images can be taken along any region, providing the cameras are above the mean water level and the horizon is clearly visible and horizontal in the viewfinder (Figure 1). If the tilt of the horizon is less than 1°, no correction for tilt is required. This is well within the visual judgment of the photographer. The available topography usually dictates the camera elevation. The authors have taken measurements at three camera elevations ranging from 8 to 24 m (depression angles ranging from 2° to 10°) and identified objects at over 600 m from the camera. Generally, for camera elevations of 10 m, measurements offshore are limited to about 250 m. The principal point of the image should be centered on the region of most interest.

For single oblique image analysis, no reference stakes are required if the horizon, the focal length of the camera lens, and the datum elevation are known. However, reference stakes are required for stereoscopic image analysis. The stereoscopic analysis requires that the principal axes of the two cameras are parallel ($\beta = 0^{\circ}$ in Figure 2). The reference stakes should be placed between the cameras. A minimum of three reference stakes are required to mathematically rotate the principal axis of one camera relative to the other camera such that $\beta = 0^{\circ}$. It is not necessary to relate the beach stakes to the camera.

If water level fluctuations are required at known points, it is suggested that plastic buoys supported by polyethylene floating rope be stretched offshore. Theoretically, this is unnecessary, but the floats provide identifiable points. This is unnecessary for the wave measurements.

III. ANALYSIS

The numerous methods of analysis of an oblique image are described in the Manual of Photogrammetry.[9] The Equivalent Vertical Photographic Method of rectifying points in the oblique image to real ground distances is well suited for surf-zone analysis. Consider an oblique image (color slide) of a plunging breaker taken along the Northern California coastline (Figure 3). The field setup is shown in Figure 1 along with several of the important points of interest such as the plunging breaker, the buoys, and the beach reference stakes. The oblique slide was enlarged using a slide projector (and photographic enlarger), and these points were digitized (Figure 4) with respect to a rectangular coordinate system with the origin at the principal point of the projected image. Fundamental relationships of an oblique image required for the analysis of this digitized image can be derived from the principal-plane diagram (Figure 5) for a slide. The plane of the positive taken by a camera lens of focal length f is defined by the points T, P, I, and N, where T is the intersection of the horizon with the principal plane, P is the principal point of the image, I is the isocenter of the image, and N is the nadir point. The depression angle, θ, is the vertical angle from the horizon plane to the optical axis. The tilt of the photograph is defined as $t = 90 - \theta$. The equivalent vertical photograph is the imaginary photograph that would be obtained if $t = 0$. The equivalent vertical photograph intersects the oblique image at the isocenter. The isoline, the line created by the intersection of the equivalent vertical photograph and the oblique image, is common to both images.

The equations required to calculate real ground distances with the origin at the camera from an oblique slide are given below. The analysis includes the effects of magnification of the slides. The magnification of the slide C is the ratio of the height of a slide, d_1, to the height of the slide on the screen, d_2, or

$$C = \frac{d_1}{d_2} . \tag{1}$$

The locations of the points P, T, I, N along the principal plane can be calculated if the positions of any two points are known. Points T and P can be measured directly from the image, and points I and N can be calculated. Then the coordinates of any point in the equivalent vertical photograph can be determined. The principal point of the enlarged oblique image is the center of the image. The distance from the principal point, P, to the apparent horizon point, T, on the slide, $\overline{PT}$, can be measured directly. The apparent depression angle, θ', is

$$\theta' = \arctan (C\,\overline{PT}/f) \quad . \qquad (2)$$

The apparent horizon is slightly lower than the true horizon, and a correction angle, $\delta\theta$, can be added to θ' to obtain the true horizon:

$$\delta\theta = 0.98(H)^{\frac{1}{2}} \quad . \qquad (3)$$

where H is in feet and $\delta\theta$ is in minutes.

Thus,

$$\theta = \theta' + \delta\theta \qquad (4)$$

and

$$\overline{PT} = f \tan\theta \quad . \qquad (5)$$

The following distances in the oblique image are given without derivation:

$$\overline{PI} = f \tan \frac{\theta}{2} \qquad (6)$$

$$\overline{PN} = f \tan \theta \qquad (7)$$

$$\overline{TI} = \overline{PT} + \overline{PI} \qquad (8)$$

$$\overline{TN} = \overline{PT} + \overline{PN} \quad . \qquad (9)$$

Using Eqs. (1) through (9), we obtain the coordinates of any point in the equivalent vertical photograph (X_{evp}, Y_{evp}), with the origin at the camera (i.e., the principal point of the equivalent vertical photograph, and not the isocenter):

$$X_{evp} = X_{ob} C \left(\frac{\overline{TI}}{\overline{TI}-K} \right) \qquad (10)$$

$$Y_{evp} = K\left(\frac{\overline{TI}}{\overline{TI}-K}\right) + \overline{NI} \tag{11}$$

where $K = Y_{ob}\,C + \overline{PI}$, $\overline{NI} = \overline{PI}$, and (X_{ob}, Y_{ob}) are the coordinates of any point on the enlarged oblique image with the origin at the principal point of the oblique image. The real ground coordinates (X_{gr}, Y_{gr}) of any point on the equivalent vertical photograph with respect to the camera are given by

$$X_{gr} = \left(\frac{H\,X_{evp}}{f}\right) \tag{12}$$

$$Y_{gr} = \left(\frac{H\,Y_{evp}}{f}\right) \tag{13}$$

where H is the difference in elevation between the camera and the point on the ground. If single images are being analyzed, H is the datum. Usually H is the difference between the elevation of the mean water level and the camera. Thus, horizontal distances can be calculated using Eqs. (12) and (13). The height of an object in a single oblique image can be calculated if the object is vertical. For vertical objects in which the bottom and top points are visible, the height, h, is given by

$$h = \frac{H(K_{top} - K_{bot})\,\overline{TN}}{\left[(TN - TI) + K_{top}\right](TI-K_{bot})} \tag{14}$$

where Y_{ob} in K_{top} is the "Y" coordinate of the top point of the vertical object and Y_{ob} in K_{bot} is the "Y" coordinate of the bottom point of the object.

If the datum fluctuates in time and space and the actual elevation of each point is of interest, then stereoscopic images are required. If two cameras with their optical axes approximately parallel are used to simultaneously take overlapping pairs of slides, then the real ground height below the camera of each point in the oblique image can be determined from parallax measurements.

The algebraic difference in the "X" coordinates of the same point in each slide of the stereo-pairs is the parallax, P, and is given by

$$P = X_{evp} - X'_{evp} \quad (15)$$

where X_{evp} and X'_{evp} are the left and right "X" coordinates on the equivalent vertical photograph. The difference in elevation between the camera and the point is given by

$$d = \frac{f\ B}{P} \quad (16)$$

where B is the baseline distance between cameras. Thus the real ground distance of any point in the oblique image is given by Eqs. (12), (13) and (16) if H = d.

IV. SINGLE-IMAGE ANALYSIS

Single oblique images can be used to measure horizontal distances such as the location of the breaker zone, nearshore wavelength, run-up on a flat beach, and ice-ridge location, using Eqs. (12) and (13) with the mean water level as the datum. For example, this method was applied to the comparison of the location of the breaker zone to the location of nearshore ice ridges found during the winter on Lake Michigan (Figure 6). These measurements are sometimes difficult to obtain by any other technique. Fluorescein dye and floats are often used to monitor the mean longshore current velocity in the nearshore zone. Consider a sequence of time-interval photographs of a dye patch at times 0, 30, and 60 s [Figures 7(a), (b), and (c), respectively]. Elaborate systems have been used to obtain vertical photographs.[3] Single oblique images can be used to make the measurements from shore. The real ground positions of the dye patch are shown in Figure 8. The mean longshore current can be calculated from the displacement of the centroid of the dye patch over time. Plunging-breaker heights can be estimated using Eq. (14). Consider the oblique image of a plunging breaker shown in Figures 3 and 9. The crest of the breaker (point A) and the intersection of the plunging breaker with the mean water level (point C) are points that can be identified on the oblique image. If the crest and the point directly below the crest (point B) could be identified, then Eq. (14) could be used directly to measure the vertical height of the wave. Although the height A-B is not a true measure of breaker height (usually defined as the difference in elevation between the crest and the trough), it does provide a good estimate. In general, point B cannot be precisely identified on images of this type. However, it is possible to estimate point B. Then, using points A and B, Eq. (14) can be applied directly. Since our estimated location of point B may not be directly below point A, an error can be expected. If the oblique image is taken when points B and C are visible along the wavefront, we can estimate the maximum possible error in the selection of point B. This possibility is considered in Figure 9. To quantify the possible error, assume that the breaker is circular. Therefore, the maximum horizontal displacement is $\frac{1}{2}H_b$. This results in an estimate of the wave height too large by $\overline{DE}$ shown in Figure 9. If a more realistic plunging-breaker shape were chosen, then a better estimate of the true plunging-breaker height would result. The above technique has been used in the field (Figure 10) and gives accurate estimates of the breaker heights.

To determine the accuracy of this simple estimate of the plunging-breaker height, a laboratory study was conducted. Circular waves 4.1, 7.7, 10.8, and 16.8 cm in diameter were constructed out of white paper. Oblique images of the paper waves similar in perspective to those found in nature were taken. The camera was kept at the same elevation but was moved farther away from the paper waves. This also changed the depression angles. The results of the experiment are shown in Figure 11. Errors of less than 5% were found. The greatest fluctuation around the mean occurred at the greatest distance from the camera because the points on the wave, such as the crest, could not be positively identified. We expect that accuracies of better than 10% can be expected routinely in the field. Further tests comparing the photographic method with wave-gauge measurements are planned.

V. STEREOSCOPIC OBLIQUE IMAGE ANALYSIS

More comprehensive measurements can be made if stereo-pairs are taken, since the vertical coordinate can be calculated directly. Thus wave height, water level fluctuations, and beach profiles can be obtained. While the single-oblique-image method can be applied at any location, providing the camera elevation above the datum is known, the stereoscopic oblique-image method requires reference stakes located between the cameras. Using the reference stakes, the angular rotation (Figure 2) of the left camera relative to the right camera can be computed. Any deviation greater than 0.1°, such that the optical axis of the left camera is not parallel to that of the right camera, will induce large errors in the analysis of the vertical coordinate using parallax. From experience, we have found that a minimum of three stakes and preferably five stakes are required. The relative elevation and distances between stakes can be surveyed simply with the stake and horizon method of Emery,[10] using standard surveying instruments. If the cameras are not parallel, the rotation error can be determined and a mathematical correction to the horizontal coordinates (X_{evp}, Y_{evp}) of an equivalent vertical photograph can be made. Assume that the left camera is oriented correctly and rotate the right camera until the absolute values of the "X" coordinates in the left and right oblique image of each reference stake add to the baseline separation difference between cameras - - i.e.,

$$B = |X_{left\ stake}| + |X_{right\ stake}| \quad . \qquad (17)$$

Due to measurement error, an average of the rotation error can be determined from three or more reference stakes. The accuracy of the correction can be determined by calculating the relative elevation and separation differences between stakes. Any rotation will result in increasing elevation errors with increasing offshore distance. The corrected equivalent vertical photograph coordinates are given by

$$X_{cevp} = X_{evp} \cos\beta + Y_{evp} \sin\beta \qquad (18)$$

$$Y_{cevp} = -X_{evp} \sin\beta + Y_{evp} \cos \qquad (19)$$

where X_{evp} and Y_{evp} are given by Eqs. (10) and (11), and β is the rotation angle.

The analysis proceeds as for the single-image analysis except that identical points must be selected in each slide (Figure 12). Identical points can be selected along the wave crest without much difficulty. However, it is not as easy to select points in the wave trough. If repeated measurements are to be made at one site, a string of buoys will provide profile lines to identify the water level at about the same point over time. An example of the water level fluctuation at two buoys separated by 8 m is given in the time series in Figure 13. If identical points are not selected in each photograph, it is usually immediately obvious, because unrealistic fluctuations occur.

VI. ERROR ANALYSIS

There are three primary sources of error in the analysis. These are:

- Measurement error
- Datum error
- Rotation error.

The measurement error is common to both the single and stereoscopic-oblique-image analyses, while the datum error affects only the single-oblique-image analysis and the rotation error affects only the stereoscopic-oblique-image analysis. There are other sources of error - - for example, due to horizontal tilt, uncertainty in the absolute focal length of the camera, uncertainty in the simultaneous exposure of the stereo-pairs, and surveying error. However, these effects are apparently negligible in the analysis.

A. Datum Error

Other than measurement error, the largest error in single-oblique-image analysis is due to the uncertainty in the datum elevation. In single-oblique-image analysis, it is assumed that all points lie on the datum. The datum in our analysis is the mean water level. Since the water surface fluctuates around the mean water level, the horizontal coordinates will have some error (Figure 14). For example, if a dye patch is determined to be 150 m from the camera at an elevation of 8 m, and the water level fluctuates ±10 cm around the mean, then the error is approximately 1 m in the offshore (Y) direction. The longshore (X) direction error is not reported, since it is not significantly affected by a datum error, and most horizontal measurements in the nearshore zone such as breaker zone, wavelength, and run-up are Y-dependent. The error in the location of a breaking wave is more critically dependent on the datum. If the amplitude of a breaking wave (crest to mean water level) located 150 m offshore is 50 cm, then an error of 7 m in the offshore distance results. However, an estimate of the amplitude of the breaker height can be made and subtracted from H to give a more realistic offshore coordinate. Therefore, a datum error of 10 cm or less can be expected for most measurements.

B. Rotation Error

Rotation primarily affects the calculation of elevation since the parallax is dependent on the "X" coordinates of an object in two oblique images. The angular rotation of one camera relative to the second required to make the line of sight of both cameras parallel is defined as β (Figure 2). If β is greater than zero degrees, an error will result. The effects of rotation error (Figure 15) increase significantly with increasing distance offshore. A relief error of over 5 m is expected at 150 m from shore if the angular rotation is 0.8°. Fortunately, the angle β can be calculated to within $\pm 0.01^{\circ}$. Therefore, these large errors are not found in the analysis. However, Figure 15 indicates how critically dependent the stereoscopic analysis is on rotation, and emphasizes the need for reference stakes on the beach.

C. Measurement Error

Measurement error is the primary source of error in our oblique-image analysis, because the analysis is done by hand and does not utilize the sophisticated equipment commonly used in aerial surveys. The measurement error includes the effects of outlining the enlarged slide frame, locating the principal point, drawing the (X_{ob}, Y_{ob}) axes through the principal point, drawing and digitizing the horizon, selecting the image point from the slide, and measuring its coordinates with a caliper. All measurements were made with a caliper accurate to ±0.001 inch. Repeated measurements indicated that an error of ±0.003 inch can be expected from any one measurement. The expected measurement error due to all the above sources was found to be about 0.015 inch. The (X_{ob}, Y_{ob}) coordinates of two different reference stakes located about 35 m from the camera were measured from 50 different oblique exposures. The standard deviation of the measurement was 0.016 and 0.015 inch, for the left and right cameras, respectively.

The effects of a possible measurement error in the X direction (ΔX) and in the Y direction (ΔY) of 0.005, 0.010, 0.015, 0.020 and 0.025 inch on the ground coordinates were calculated for three locations. The error analysis was applied at the reference stakes (35 m), the offshore buoys used to calculate mean water (50 m), and the breaking wave (150 m) in Figure 1. Corrected datum levels were used in the calculation. The results are shown in Figures 16 through 20.

The error in estimating a plunging-breaker height by single-oblique-image analysis 150 m from the camera is shown in Figure 16. A total measurement error of 0.015 inch in determining the Y_{ob} coordinate would result in a 15-cm error. This error includes the effects of selecting the points from the image, including the uncertainty of selecting the trough. Since the computation depends on the difference between two "Y_{ob}" coordinates, and the major portion of the 0.015-inch error is a constant bias and not a random error for this calculation, better accuracies are possible.

The possible measurement errors in the longshore (X) and offshore (Y) directions for single oblique images are shown in Figures 17 and 18. Measurement error is linear in the X direction and negligible over the range of offshore distances assumed in the analysis. Although the error in the offshore distance is larger than the error in the longshore direction, it too is small. For example, a measurement error of 0.015 inch in a wave 150 m from shore results in an error of about 3 m. This is about 2%, which is sufficiently accurate for most measurements.

The range of possible relief errors for stereoscopic oblique image analysis due to measurement errors in X_{ob} and Y_{ob} is shown in Figures 19 and 20. Since the calculation of X_{evp} in Eq. (10) is dependent on the calculation of Y_{evp}, the measurement errors in the Y_{ob} direction will effect the parallax. In fact, for increasing offshore distances the effect of ΔY measurement errors increases until it affects the parallax more rapidly than do ΔX measurement errors.

For offshore distances greater than 150 m, the relief errors are more dependent on ΔY measurement errors than on ΔX measurement errors. The family of curves in Figure 19 would be linear if the same datum were assumed for all calculations.

V11. CONCLUSION

Single- and stereoscopic-oblique-image analysis can be used to monitor waves, water level, and longshore currents in the nearshore zone using a 35-mm camera, a tripod, and a slide projector. Accuracies of 10% or better can be attained for these measurements. This technique should find application in coastal monitoring programs.

Acknowledgments. The authors would like to express their appreciation to Messrs. C. Carlson, J. Maresca, Sr., G. Springer, C. Vogelsang, and W. Zavoli for their assistance in the field experiments. We express appreciation for Mr. C. T. Carlson's efforts in assisting in developing and refining this technique for application to nearshore ice studies on Lake Michigan. We would also like to thank Dr. C. Olson for his encouragement and helpful discussions on analysis of oblique images.

REFERENCES

1. D. D. Stafford, R. O. Bruno, and H. M. Goldstein, "An Annotated Bibliography of Aerial Remote Sensing in Coastal Engineering," MP 2-73, Coastal Engineering Research Center, Fort Belvoir, Va. (1973).
2. L. J. Cote, J. O. Davis, W. Marks, R. J. McGough, E. Mehr, W. J. Pierson, Jr., J. F. Ropek, G. Stephenson, and R. C. Vetter, "The Directional Spectrum of a Wind Generated Sea as Determined from Data Obtained by the Stereo Wave Observation Project," Meteorol. Papers, Vol. 2, No. 6, NYU College of Engineering, New York City (1960).
3. C. J. Sonu, "Tethered Balloon for Study of Coastal Dynamics," Proc. Symposium Earth Observation Balloons, pp. 91-102 (1969).
4. E. C. Monahan, "Fresh Water Whitecaps," J. Atmos. Sci., Vol. 26, No. 5, pp. 1026-29 (1969).
5. J. W. Maresca, Jr., "Bluffline Recession, Beach Change and Nearshore Change Related to Storm Passages Along Southeastern Lake Michigan," Ph.D. Dissertation, University of Michigan, Ann Arbor, Michigan (1975).
6. E. Seibel, C. T. Carlson, and J. W. Maresca, Jr., "Lake and Shore Ice Conditions on Southeastern Lake Michigan in the Vicinity of the Donald C. Cook Nuclear Plant: Winter 1973-1974. Part XXI," Special Report No. 55, Great Lakes Research Division, University of Michigan, Ann Arbor, Michigan (1975).
7. E. Seibel, C. T. Carlson, and J. W. Maresca, Jr., "The Interrelationship between Nearshore Ice Ridges, Breaking Waves, and Offshore Bars Along Southeastern Lake Michigan," accepted for publication in Great Lakes Res. (1976).
8. H. J. Pincus, "Some Application of Terrestrial Photogrammetry to the Study of Shorelines," Photogrammetric Eng., Vol. 25, No. 3, pp. 75-82 (March 1959).
9. American Society of Photogrammetry, Manual of Photogrammetry, 3rd Ed., Washington, D.C. (1966).
10. K. O. Emery, "A Simple Method of Measuring Beach Profiles," Limnology and Oceanography, Vol. 6, pp. 90-93 (1961).

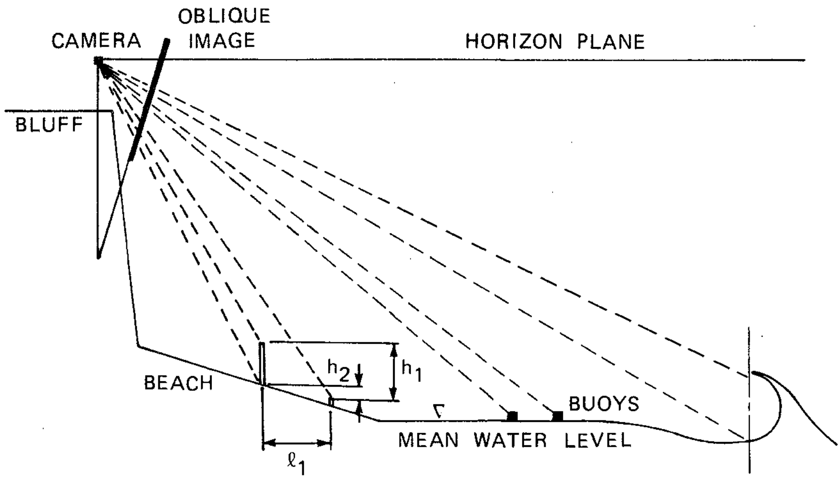

FIGURE 1 OBLIQUE IMAGERY OF THE SURF ZONE

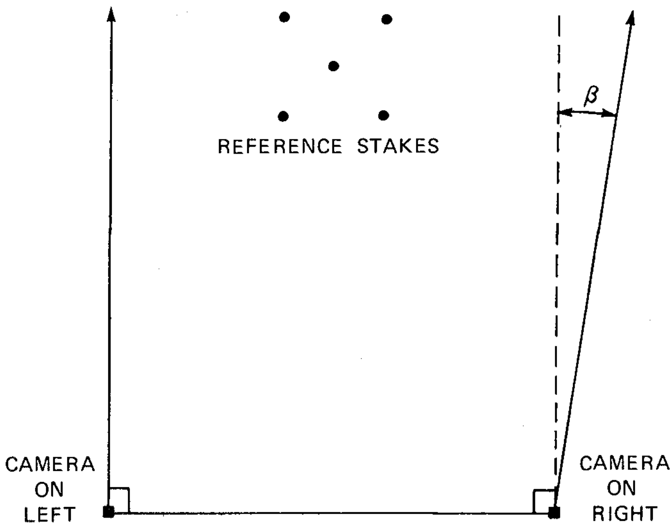

FIGURE 2 EFFECT OF ROTATION ERROR ON STEREOSCOPIC OBLIQUE ANALYSIS. The actual optical axes of the cameras are denoted by the solid line. If β = 0, the optical axes of the cameras are parallel.

FIGURE 3 SINGLE OBLIQUE IMAGE OF A PLUNGING BREAKER, BUOYS, AND REFERENCE STAKES, AS ILLUSTRATED IN FIGURE 1

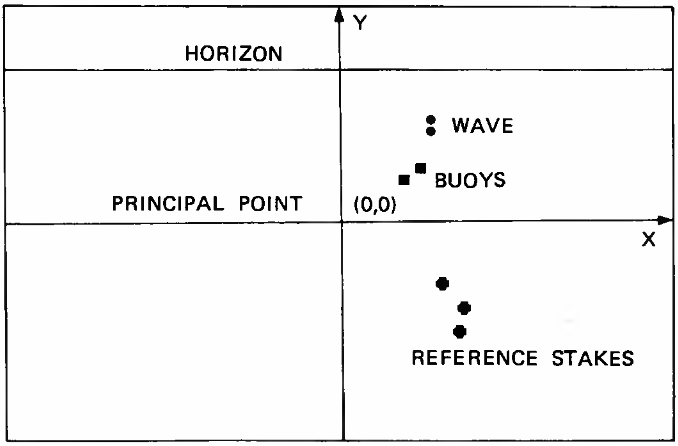

FIGURE 4 DIGITIZED SINGLE OBLIQUE IMAGE

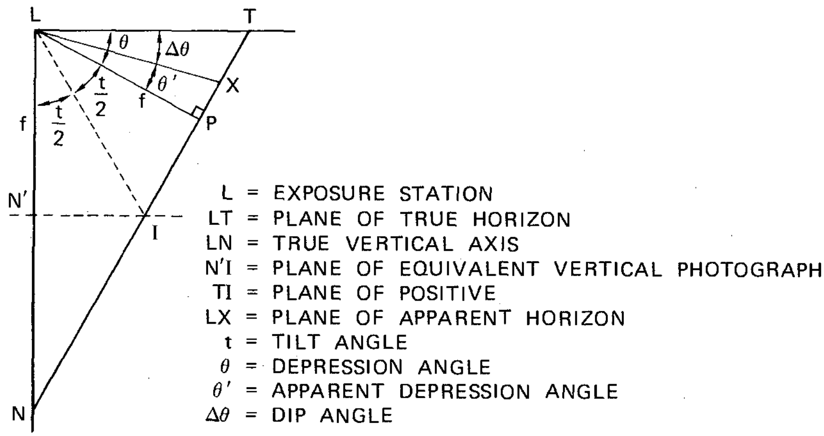

FIGURE 5 PRINCIPAL-PLANE DIAGRAM

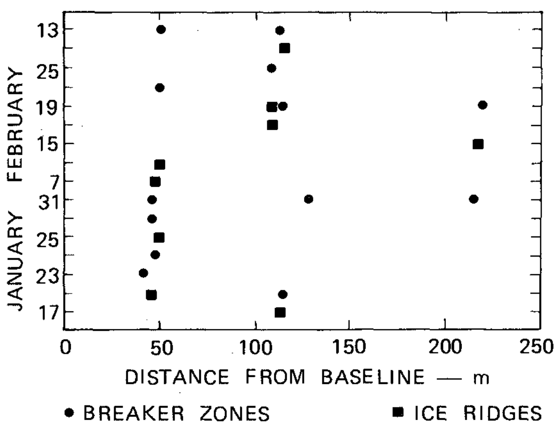

FIGURE 6 LOCATION OF ICE RIDGES AND BREAKER ZONES FOR SINGLE OBLIQUE IMAGES

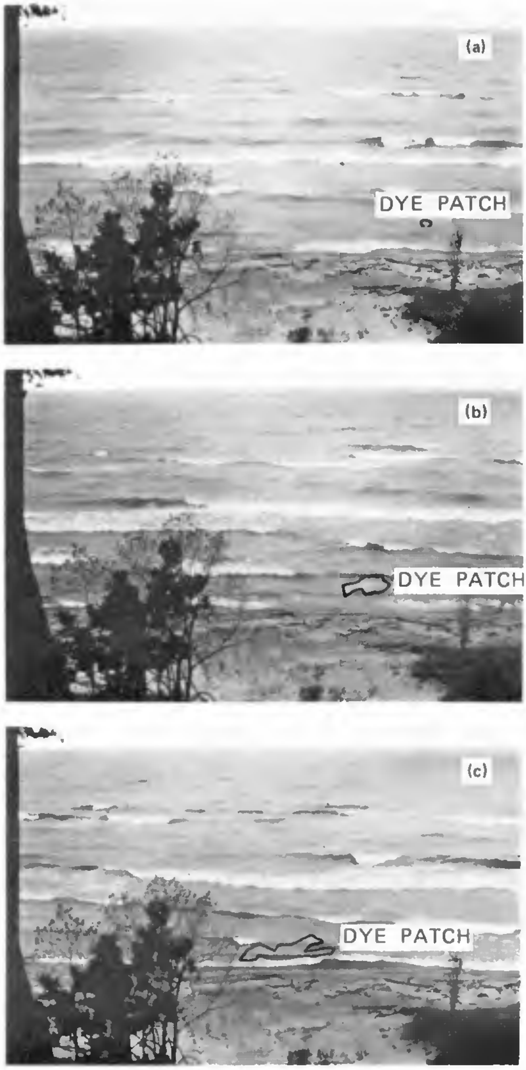

FIGURE 7 SINGLE OBLIQUE IMAGE OF A FLUORESCEIN DYE PATCH. (a) At time of release, (b) 30 s after release, (c) 60 s after release.

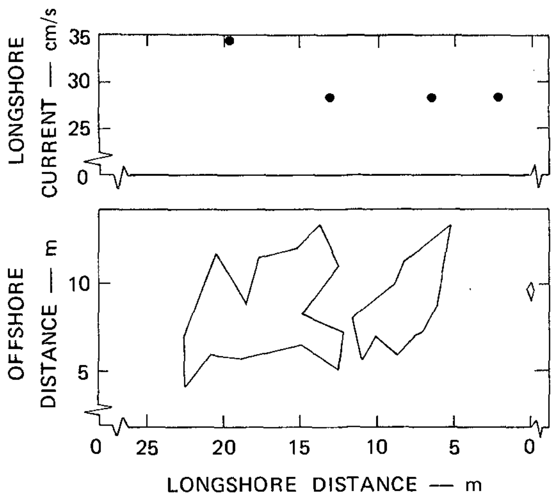

FIGURE 8 SINGLE-OBLIQUE-IMAGE ANALYSIS OF THE LONGSHORE CURRENT

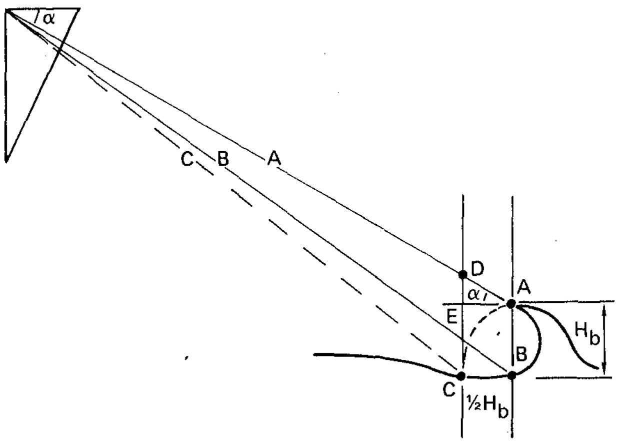

FIGURE 9 DEFINITION OF PLUNGING-BREAKER HEIGHT. Breaker height is defined as $\overline{AB}$. If points A and C are used to calculate the breaker height, then the breaker height is $\overline{DC}$. The error is $\overline{DE} = \overline{EA} \tan \alpha = 1/2\ H_b \tan \alpha$.

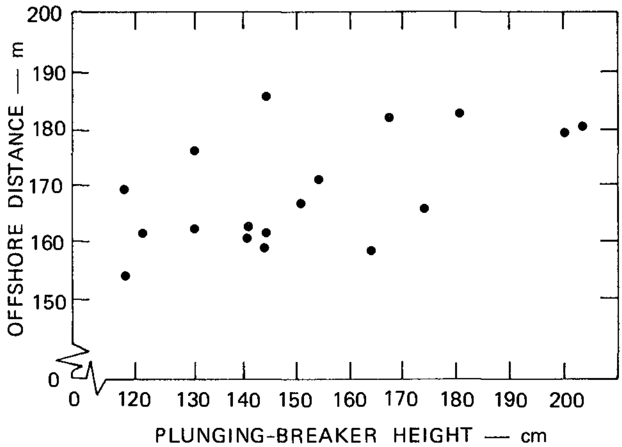

FIGURE 10 SINGLE-OBLIQUE-IMAGE ANALYSIS OF PLUNGING-BREAKER HEIGHTS IN THE FIELD

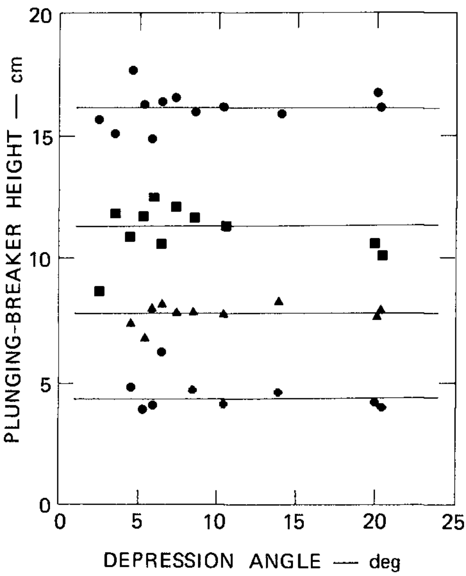

FIGURE 11 SINGLE-OBLIQUE-IMAGE ANALYSIS OF PLUNGING-BREAKER HEIGHTS IN THE LABORATORY

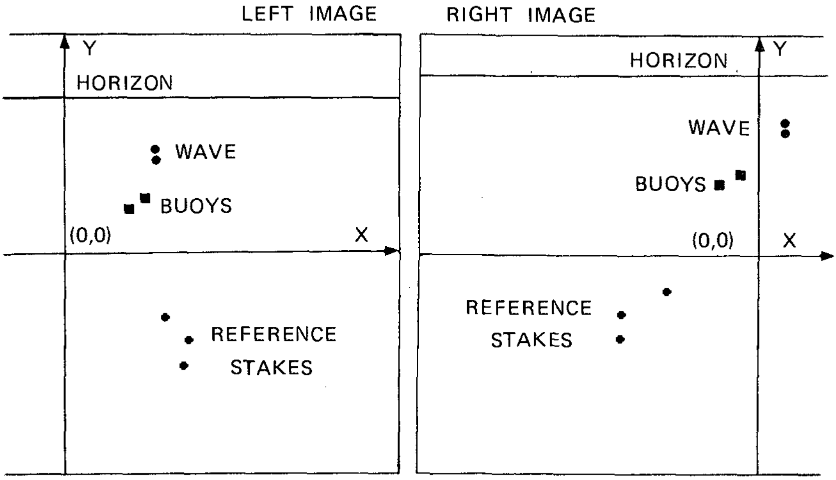

FIGURE 12 DIGITIZED STEREOSCOPIC OBLIQUE IMAGES

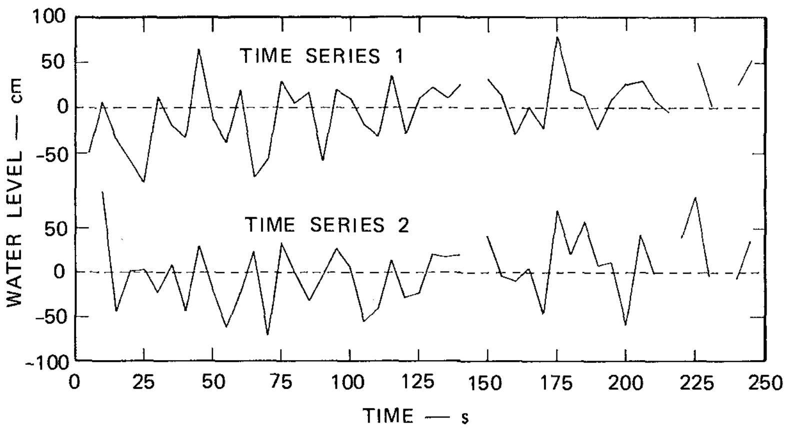

FIGURE 13 WATER LEVEL FLUCTUATION BY STEREOSCOPIC-OBLIQUE-IMAGE ANALYSIS

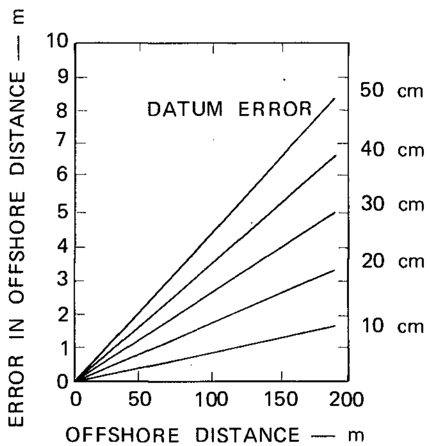

FIGURE 14 ERROR IN OFFSHORE DISTANCE DUE TO DATUM ERROR FOR SINGLE OBLIQUE IMAGE

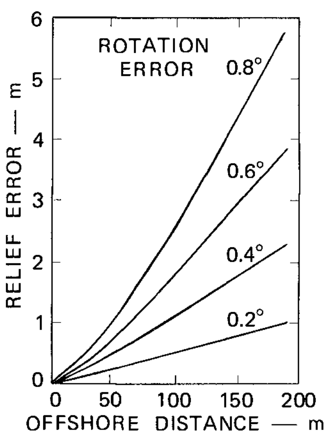

FIGURE 15 RELIEF ERROR DUE TO ROTATION ERROR FOR STEREOSCOPIC OBLIQUE ANALYSIS

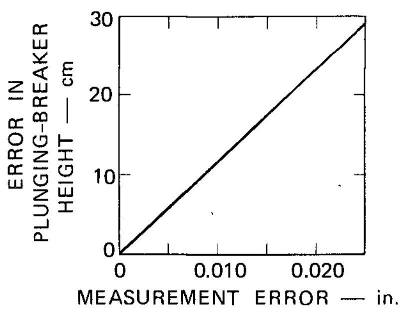

FIGURE 16 ERROR IN PLUNGING-BREAKER HEIGHT FOR SINGLE-OBLIQUE-IMAGE ANALYSIS

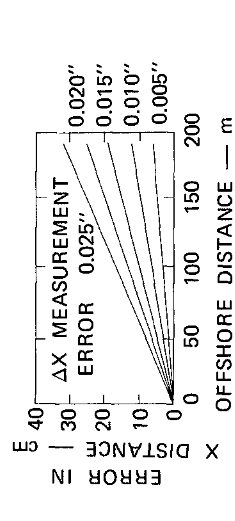

FIGURE 17 ERROR IN X DISTANCE DUE TO ΔX MEASUREMENT ERROR FOR SINGLE OBLIQUE IMAGE

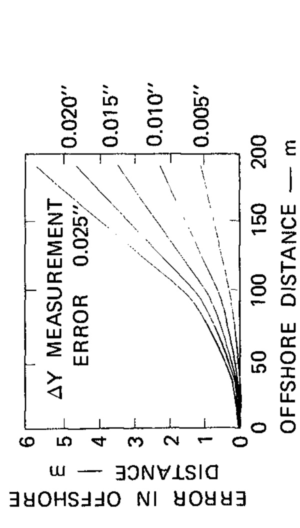

FIGURE 18 ERROR IN OFFSHORE DISTANCE DUE TO ΔY MEASUREMENT ERROR FOR SINGLE OBLIQUE IMAGE

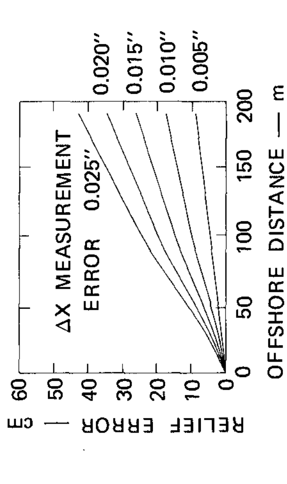

FIGURE 19 RELIEF ERROR DUE TO ΔX MEASUREMENT ERROR FOR STEREOSCOPIC OBLIQUE ANALYSIS

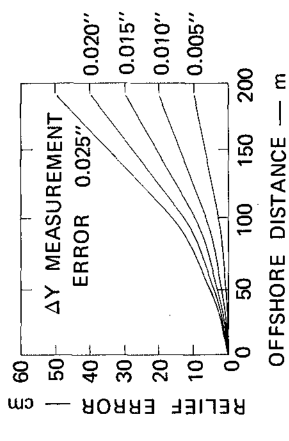

FIGURE 20 RELIEF ERROR DUE TO ΔY MEASUREMENT ERROR FOR STEREOSCOPIC ANALYSIS